Fusion Engineering and Design 89 (2014) 2150–2154

Contents lists available at ScienceDirect

Fusion Engineering and Design

journal homepage: www.elsevier.com/locate/fusengdes

Operational characteristics of the high flux plasma generator Magnum-PSI

H.J.N. van Eck[a,*], T. Abrams[b], M.A. van den Berg[a], S. Brons[a], G.G. van Eden[a], M.A. Jaworski[b], R. Kaita[b], H.J. van der Meiden[a], T.W. Morgan[a], M.J. van de Pol[a], J. Scholten[a], P.H.M. Smeets[a], G. De Temmerman[a], P.C. de Vries[a], P.A. Zeijlmans van Emmichoven[a]

[a] FOM Institute DIFFER, Dutch Institute For Fundamental Energy Research, Association EURATOM-FOM, Trilateral Euregio Cluster, P.O. Box 1207, 3430 BE Nieuwegein, The Netherlands
[b] Princeton Plasma Physics Laboratory, Princeton, NJ 08543, USA

HIGHLIGHTS

- We have described the design and capabilities of the plasma experiment Magnum-PSI.
- The plasma conditions are well suited for PSI studies in support of ITER.
- Quasi steady state heat fluxes over 10 MW m^{-2} have been achieved.
- Transient heat and particle loads can be generated to simulate ELM instabilities.
- Lithium coating can be applied to the surfaces of samples under vacuum.

ARTICLE INFO

Article history:
Received 13 September 2013
Received in revised form 6 March 2014
Accepted 22 April 2014
Available online 15 May 2014

Keywords:
ITER
Plasma–surface interactions
ELMs
Linear plasma device
Lithium coatings

ABSTRACT

In Magnum-PSI (MAgnetized plasma Generator and NUMerical modeling for Plasma Surface Interactions), the high density, low temperature plasma of a wall stabilized dc cascaded arc is confined to a magnetized plasma beam by a quasi-steady state axial magnetic field up to 1.3 T. It aims at conditions that enable fundamental studies of plasma–surface interactions in the regime relevant for fusion reactors such as ITER: 10^{23}–10^{25} m^{-2} s^{-1} hydrogen plasma flux densities at 1–5 eV. To study the effects of transient heat loads on a plasma-facing surface, a high power pulsed magnetized arc discharge has been developed. Additionally, the target surface can be transiently heated with a pulsed laser system during plasma exposure. In this contribution, the current status, capabilities and performance of Magnum-PSI are presented.

1. Introduction

Whereas ITER, in terms of plasma temperature and density, is very similar to JET, it represents a huge upscale in terms of plasma–wall interaction, because the flux densities are an order of magnitude higher while the pulse length exceeds that of JET by eventually up to two orders of magnitude. The stored energy in the plasma of ITER ($W_{plasma} \sim 350$ MJ) is more than a factor 30 above of what is currently achievable in JET ($W_{plasma} \sim 10$ MJ), and the combination of long-pulse, large size, and high density operation in ITER will give a 3-orders-of-magnitude increase in the ion fluence to the divertor. As a result, one ITER shot (~400 s) equals approximately three years of normal JET operation in terms of ion fluence to the divertor [1]. On top of that, the divertor strike zones will experience elevated heat and particle fluxes as a result of instabilities in the plasma edge, commonly called Edge Localized Modes (ELMs). During such an ELM, the heat and particle fluxes to the divertor can exceed the damage threshold of the wall material for a short time (sub-ms). No existing toroidal confinement device can reach these

* Corresponding author. Tel.: +31 306096760.
E-mail address: h.j.n.vaneck@differ.nl (H.J.N. van Eck).

http://dx.doi.org/10.1016/j.fusengdes.2014.04.054
0920-3796/

intense transient heat loads predicted for ITER by a large margin [2].

In order to address the complex physics of the ITER divertor in a systematic way, with controlled plasma parameters, flexible target geometry and good diagnostic access, the Dutch Institute For Fundamental Energy Research (FOM Institute DIFFER) decided to develop a new experiment with the relevant PSI parameters. This apparatus, Magnum-PSI (MAgnetized plasma Generator and NUMerical modeling for Plasma Surface Interaction) consists of a linear plasma generator equipped with a superconducting magnet to allow for continuous exposure. For the plasma source, the cascaded arc [3] was chosen as the best way to produce the high hydrogen plasma flux that is required, at a plasma temperature in the eV range. However, this type of source co-injects a large neutral gas flow into the vacuum vessel due to its finite ionization efficiency. The need for a relatively low neutral pressure at the target has led to the implementation of a differentially pumped vacuum vessel, which is divided into three individually pumped chambers. Flow restrictions (skimmers) between the vacuum chambers keep the neutral gas flow to the target low enough without hampering the plasma flow [4]. The steady state high magnetic field is needed to confine the plasma beam in the first place, but also critically determines the magnetization of the plasma near the target, and thereby the recycling. A field strength of the same order as that in ITER was called for without hampering the diagnostic access to the machine.

For the development of Magnum-PSI, to test concepts, develop the source technology and to benchmark numerical calculations, a forerunner experiment was set up: Pilot-PSI. It is smaller in dimension and uses five oil-cooled Bitter coils to generate pulsed magnetic fields between 0.4 and 1.6 T. With this setup, ITER relevant plasma parameters were reached, with corresponding ion flux densities up to 10^{25} m^{-2} s^{-1} in a full-width-half-maximum (FWHM) beam diameter of 1 cm [5]. A capacitor bank connected in parallel to the steady state power supplies of the plasma source can be used to superimpose power transients, pushing the ion flux density beyond 10^{26} m^{-2} s^{-1} for about 1 ms [6,7].

In this contribution, the design values, current status and operational characteristics of the Magnum-PSI device are presented.

2. Technical implementation

2.1. Design philosophy

The choice of system parameters for the Magnum-PSI experiment is focused on reaching the ITER relevant regime of PSI. The design philosophy was to strive for maximum flexibility to be able to adapt to new physics insights. This has led to a modular design, where each component can be modified without having a large impact on the rest of the machine. More specifically: the large diameter magnet creates space for diagnostics, while the variable magnetic field strength is strong enough not to restrict the operational space. The water cooled, movable target holder can accommodate targets of different sizes and composition, and allows the targets to be biased to vary the energy of the incoming particles. The variable pumping speed has a maximum that is high enough to keep the neutral pressure in the target region below 1 Pa during plasma exposure. The plasma source is mounted in a movable tube, to allow for source exchange and variation of its position with respect to the target and magnetic field. A wide range of plasma parameters can be achieved by varying gas flow, source current, magnetic field and target bias. In Fig. 1, a side view of the experiment can be seen. More information about the construction can be found in Ref. [8].

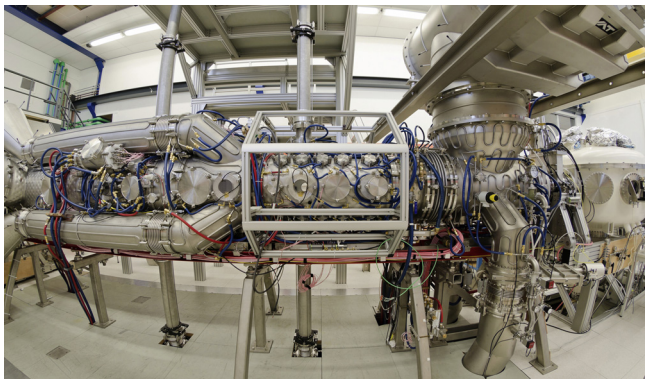

Fig. 1. Side view of the Magnum-PSI experiment. The cascaded arc plasma source is located inside the left chamber of the water cooled differentially pumped vacuum vessel. The target is exposed to the plasma beam in the vacuum chamber fitted with many diagnostic ports in the middle of the picture. After exposure, the target can be transferred under vacuum to the white surface analysis station on the far right. The total length of the set-up is 18 m. The picture was taken before installation of the electromagnets.

2.2. Design values

The most important design parameters in terms of performance can be summarized as:

- Plasma parameters relevant to high performance detached divertor operation in ITER:
  - electron density $n_e \sim 10^{19}$–10^{21} m^{-3}
  - electron temperature $T_e \sim 0.1$–10 eV
  - particle flux $\sim 10^{23}$–10^{25} m^{-2} s^{-1}
- Heat fluxes > 10 MW m^{-2}
- Low neutral background density < 1 Pa
- Strong magnetic field up to 2.5 T
- Inclined (2.9–90° with respect to the plasma beam) targets with a maximum size of 0.1×0.6 m^2
- Cooling power of the target up to 100 kW
- High fluence/long timescale due to steady state capability
- Transient plasma loading capability up to 1 GW m^{-2} with a variable repetition rate > 100 Hz.

2.3. Diagnostics

One of the key aspects of the experiment is its diagnostic access, which allows for many different plasma and surface diagnostics to be installed. The most important plasma diagnostic is Thomson Scattering (TS), which determines n_e and T_e profiles downstream from the source exit and directly in front of the target with a spatial resolution of 1.6 mm [9] and a repetition period of 1 s. The minimum measurable n_e and T_e values are $\sim 1 \times 10^{17}$ m^{-3} and $\sim$0.07 eV, respectively. The accuracy of n_e and T_e is 3% and 6%, respectively, at $n_e = 9.4 \times 10^{18}$ m^{-3}. By virtue of the high sensitivity of the system, single pulse TS has been successfully applied on plasmas generated during transient heat load experiments with a repetition period of 200 ms, limited by the ICCD camera read-out speed. Information on the composition of the plasma in front of the target is obtained from wide spectral range optical emission spectroscopy (OES), while high resolution OES delivers information on velocity of the ions, and indirectly on their temperature.

For a direct measurement of the ion temperature T_i and flow velocity of the plasma v_{plasma}, a Collective TS system (CTS) is being built. Forward CTS, based on a seeded Nd:YAG laser operating at 1064 nm, can be applied at Magnum-PSI to measure T_i and v_{plasma} unambiguously with an accuracy of <8% and <15%, respectively [10]. Two high spectral resolution (<0.005 nm) detection schemes are

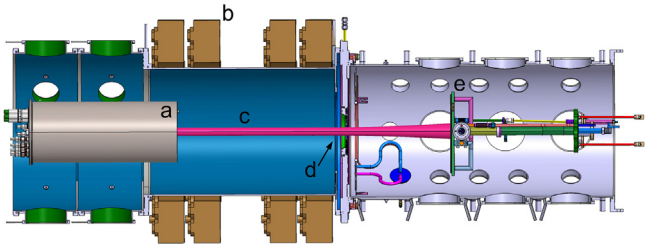

Fig. 2. Design drawing of the current status of the Magnum-PSI experiment. The cascaded arc plasma source (a) is located inside the left chamber of the water cooled differentially pumped vacuum vessel. The output of the source is confined to a beam by an axial magnetic field generated by Bitter coils (b). The magnetized plasma beam (c) flows through the skimmer (d) from source to target (e) while most of the neutrals are scraped off and pumped away. The distance between the source and the target is 1 m. The target can be rotated around two orthogonal axes to vary the angle of incidence.

applied simultaneously: an Echelle grating spectrometer (enabling profile measurements) and a system based on a Fabry–Perot etalon that enables wavelength scanning over its free spectral range, by tilting the device.

It is important to be able to monitor some of the surface properties during operation (*in situ*) to have a means of control. A fast infrared camera (FLIR SC7500-MB) with a frame rate of 30 kHz, together with a multi-wavelength spectroscopic pyrometer (FAR Spectro Pyrometer model FMPI), are used to measure the 2D distribution of the surface temperature [11]. A fast visible light camera (Phantom) with a frame rate up to 1 MHz is available for monitoring short lived events or fluctuations. Temperature and flow sensors are installed inside the cooling circuits to determine the heat load to the target. To further determine the properties of the surface which are modified in the interaction with the plasma, the target can be retracted under vacuum into the TEAC. The ex situ diagnostics installed there include Laser Induced Desorption combined with a Quadrupole Mass Spectrometer (LID–QMS: for deuterium retention measurements) and Laser Induced Breakdown Spectroscopy (LIBS: for surface composition with a depth resolution of about 200 nm). With LID, a millisecond pulse, high intensity laser beam irradiates a spot on the target leading to desorption of deuterium out of the material while minimizing surface changes.

Thermal Desorption Spectroscopy (TDS) and X-ray Photoelectron Spectroscopy (XPS) are available ex situ at a nearby location.

2.4. Current status

Due to a significant delay in the delivery of the superconducting magnet it was decided to implement a temporary contingency plan in which a magnetic field is generated with conventional electromagnets. These oil-cooled Bitter coils generate a magnetic field up to 1.3 T near the source for 12 s, with the pulse time being limited by Ohmic heating of the coils. The magnetic field can be stepwise lowered down to 0.43 T, enabling longer pulse times up to 112 s. The coils are positioned such that the magnetic field lines expand a factor of 2.6 in diameter before reaching the target. A schematic overview of the current status of the Magnum-PSI experiment is shown in Fig. 2.

The experiment uses a two stage differentially pumped vacuum system to keep the influx of cold neutrals from the source in the target region low enough. In the current configuration the gas injection rate can be varied between roughly 5 and 25 Pa m^3 s^{-1}. The vacuum chambers are separated by a skimmer and each chamber is pumped by its own pumping station consisting of large roots blowers with an effective pump speed ~20.000 m^3 h^{-1} between 1 and 80 Pa. With this configuration, it was confirmed that the neutral flux to the target is much lower than the incoming ion flux [12].

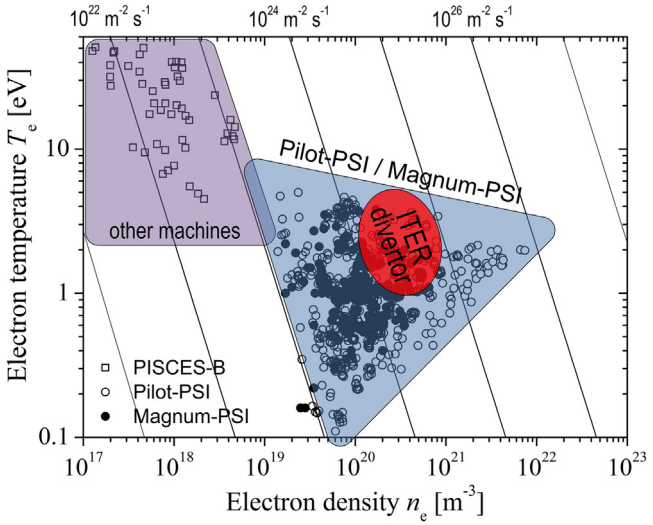

Fig. 3. Representation of the parameter space of electron density and temperature for the linear plasma generators available for fusion research, in comparison to the plasma parameters expected at the divertor strike zones for ITER. All points are for hydrogen. Diagonal solid lines of constant flux density are given.

3. Operations

3.1. Operational range

In Fig. 3 the parameter space of n_e and T_e for the linear plasma generators available for fusion research are compared to the plasma parameters expected at the divertor strike zones for ITER [13] ($n_e \sim 10^{20}$–10^{21} m^{-3} and $T_e \sim 1$–5 eV with a resulting particle and heat flux of ~10^{24} m^{-2} s^{-1} and ~10 MW m^{-2}, respectively). The linear machines indicated with "other machines" include the PISCES-B facility at the University of California in San Diego [14], which is capable of handling Beryllium targets relevant for the first wall of ITER, the JULE-PSI experiment in Juelich [15] (based on PSI-2, formerly at the Humboldt University in Berlin [16]), capable of handling neutron activated and toxic targets, and NAGDIS-II at Nagoya University [17].

The solid black data points were measured during the commissioning phase of the Magnum-PSI facility. The data points represented with open circles are measured on Pilot-PSI and taken from Ref. [18]. The blue triangle is a rough indication of the parameter space which can be achieved by changing the gas flow, source current and magnetic field. No target bias was applied. The parameter space for the other machines is derived from Refs. [14,16,17], with the open squares valid for the PISCES-B facility. All data points are for H_2. The flux density was calculated according to the Bohm criterion [19] assuming the density at the sheath edge is half the upstream density. The solid black diagonal lines represent a constant flux density.

In the present configuration of Magnum-PSI, the parameter space is limited due to the expanding magnetic field at the target region. The magnetic geometry broadens the plasma beam, which reduces the plasma density and temperature. As a consequence, also the heat flux is limited in the existing situation. Peak heat fluxes over 10 MW m^{-2} have been reached with a source current of 250 A and a magnetic field of 1.4 T [12,20], while heat fluxes up to 50 MW m^{-2} were achieved in Pilot-PSI [21].

After installation of the superconducting magnet, the parameter space for Magnum-PSI is expected to expand to the area roughly indicated with the blue triangle. The requirement for an ITER-relevant particle flux of ~10^{24} m^{-2} s^{-1} on a target under grazing incidence translates to a parallel particle flux requirement of

$\sim 10^{25}$ m^{-2} s^{-1}. This is the reason for data point showing higher fluxes than given for the ITER divertor region. The plasma parameters from Pilot-PSI and Magnum-PSI are suited for PSI studies in the ITER divertor relevant regime.

3.2. Transient heat loads

To simulate the transient heat and particle loads onto the divertor as they occur during an ELM instability in a tokamak, a high power pulsed magnetized arc discharge has been developed by utilizing a set of coupled capacitor banks discharged through the source. This permits a >100 Hz repetition rate for peak heat fluxes currently of 0.1–0.15 GW m^{-2} limited mainly by the magnetic flux expansion at the target [22]. Due to the high n_e produced by the discharge, single-pulse Thomson scattering is possible, and electron densities and temperatures during the pulse were achieved up to $n_e \approx 1.2 \times 10^{21}$ m^{-3} and $T_e \approx 6$ eV at the target position. The current rise time is 200–300 μs while the pulse duration is 0.7–1.5 ms. The pulse can be shaped by changing the delay of capacitor sections or the number of capacitors discharged together to maximize flexibility and well-replicate ELM heat flux evolutions. The peak heat fluxes and electron densities are around a factor 5 lower than those achieved in Pilot-PSI [23] leading to a correspondingly smaller temperature rise. This can be attributed to the expansion of the magnetic field which is a factor 10 lower at the target position than in Pilot-PSI. With the implementation of superconducting coils, ITER relevant heat fluxes well in excess of 1 GW m^{-2} are expected to be achieved.

Additionally, the target surface can be heated with a pulsed laser system during plasma exposure. A 1064 nm high power Nd:YAG laser is coupled to the target chamber and delivers laser pulses with a heat flux parameter up to 50 MW m^{-2} s$^{1/2}$. The spot size is about 3 mm^2, and the pulse duration can be varied between 0.5 and 5 ms with a frequency up to 25 Hz. This pulse length and laser operating frequency match the expected type-1 ELMs in ITER (0.1–1 ms pulse length ~1–10 Hz [24,25]) more realistically than previous laser heat load experiments on tungsten [26–28] and provides similar capabilities as those available at PISCES-B [29]. The resulting heat flux is high enough to repeatedly bring a tungsten surface briefly above its melting point (T_m = 3422 °C). A typical surface temperature response of a tungsten target exposed to a laser pulse during plasma exposure is shown in Fig. 4.

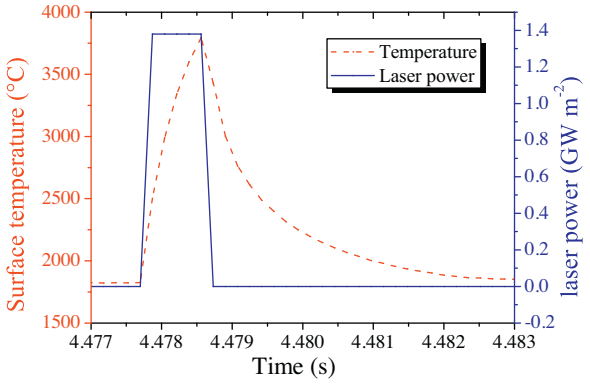

Fig. 4. Surface temperature response of a tungsten target, as determined from a fast IR camera, exposed to a laser pulse during plasma exposure. The laser power was calculated from the transmitted laser energy and pulse length, the laser spot size as determined both from laser paper and IR camera observations and the reflectivity of the surface as determined by ellipsometry.

3.3. Preparation of lithium coatings

Liquid metals could potentially provide an alternative for solid metal plasma-facing components (PFCs). Their principal operation is based on the "self-healing" nature of a liquid in which new material flows in, thereby renewing the surface and mitigating any plasma-induced damage effects. In addition, the liquid material can be used to decouple the effects related to plasma and neutron exposure, i.e. no single material needs to deal with the high heat fluxes and neutron irradiation at the same time. A novel divertor configuration where the incident heat flux to the PFC is mitigated by continuous vapor-shielding offers great promises but should first be studied in a realistic environment with a high plasma density, like in Magnum-PSI.

Lithium coatings can now be applied to the surfaces of samples in the TEAC with the use of the LITER-1C lithium evaporator. The LITER-1C was one of a series of prototype evaporators developed for the NSTX boundary physics program [30]. The LITER-1C is an effusion oven with a maximum capacity of 100 g of lithium depending on orientation. Previous evaporators had capacities of about 25 mg necessitating frequent re-loadings. The LITER-1C has an open aperture of about 285 mm^2 and can routinely achieve lithium deposition rates of 30 nm/min at the target location (characterized with a quartz–crystal deposition monitor assuming a nominal lithium density of 0.53 g/cc). A set of gate valves allow the evaporator to remain at stand-by temperatures while the sample is exposed to the Magnum-PSI plasma discharges.

The system has been used to deposit Li coatings on Mo and graphite up to 1 μ in thickness. During plasma exposure, Li I emission was captured by 2D fast-filtered imaging and spectroscopy. The experiment was designed to measure the gross erosion rate and re-deposition fraction and to investigate the vapor-shielded regime.

4. Conclusions

The design parameters of Magnum-PSI and their technical implementation in terms of performance and analysis make the device a well suited facility for PSI research in support of ITER and fusion reactors beyond ITER. In this contribution, we have described the design, current status and capabilities of the device. Although, the parameter space in terms of plasma density, heat flux and pulse duration is currently limited by the use of conventional electromagnets, quasi steady state heat fluxes over 10 MW m^{-2} have already been achieved. In addition, a capacitor bank system has been developed to superimpose ELM-like plasma pulses to the steady state plasma with a repetition rate > 100 Hz. Furthermore, the target under exposure can be transiently heated by a high power laser system. The LITER-1C effusion oven can be used to apply Lithium coatings to the surfaces of samples in the TEAC.

Acknowledgments

This work, supported by the European Communities under the contract of the Association EURATOM/FOM, was carried out within the framework of the European Fusion Programme with financial support from NWO. The views and opinions expressed herein do not necessarily reflect those of the European Commission.

References

[1] R.A. Pitts, J.P. Coad, D.P. Coster, G. Federici, W. Fundamenski, J. Horacek, et al., Plasma Phys. Control. Fusion 47 (2005) B303.
[2] T. Eich, A. Herrmann, G. Pautasso, P. Andrew, N. Asakura, J.A. Boedo, et al., J. Nucl. Mater. 337–339 (2005) 669.
[3] M.C.M. van de Sanden, G.M. Janssen, J.M. de Regt, D.C. Schram, J.A.M. van der Mullen, B. van der Sijde, Rev. Sci. Instrum. 63 (1992) 3369.

[4] H.J.N. van Eck, W.R. Koppers, G.J. van Rooij, W.J. Goedheer, R. Engeln, D.C. Schram, et al., J. Appl. Phys. 105 (2009) 063307.
[5] G.J. van Rooij, V.P. Veremiyenko, W.J. Goedheer, B. de Groot, A.W. Kleyn, P.H.M. Smeets, et al., Appl. Phys. Lett. 90 (2007) 121501.
[6] G. De Temmerman, J.J. Zielinski, H. van der Meiden, W. Melissen, J. Rapp, Appl. Phys. Lett. 97 (2010) 081502.
[7] G. De Temmerman, J. Zielinski, S. van Diepen, L. Marot, M. Price, Nucl. Fusion 51 (2011) 073008.
[8] J. Rapp, W.R. Koppers, H.J.N. van Eck, G.J. van Rooij, W.J. Goedheer, B. de Groot, et al., Fusion Eng. Des. 85 (2010) 1455.
[9] H.J. van der Meiden, A.R. Lof, M.A. van den Berg, S. Brons, A.J.H. Donné, H.J.N. van Eck, et al., Rev. Sci. Instrum. 83 (2012) 123505.
[10] H.J. van der Meiden, Plasma Phys. Control. Fusion 52 (2010) 045009.
[11] M.A. van den Berg, K. Bystrov, R. Pasquet, J.J. Zielinski, G. De Temmerman, J. Nucl. Mater. 438 (2013) S431.
[12] H.J.N. van Eck, A.W. Kleyn, A. Lof, H.J. van der Meiden, G.J. van Rooij, J. Scholten, et al., Appl. Phys. Lett. 101 (2012) 224107.
[13] A.S. Kukushkin, H.D. Pacher, A. Loarte, V. Komarov, V. Kotov, M. Merola, et al., Nucl. Fusion 49 (2009) 075008.
[14] Y. Hirooka, R.W. Conn, T. Sketchley, W.K. Leung, G. Chevalier, R. Doerner, et al., J. Vac. Sci. Technol. A 8 (1990) 1790.
[15] B. Unterberg, R. Jaspers, R. Koch, V. Massaut, J. Rapp, D. Reiter, et al., Fusion Eng. Des. 86 (2011) 1797.
[16] H. Grote, W. Bohmeyer, H. Reiner, H. Behrendt, G. Fussmann, H. Meyer, et al., J. Nucl. Mater. 241–243 (1997) 1152.
[17] E.M. Hollmann, D.G. Whyte, D. Nishijima, N. Ohno, Y. Uesugi, N. Ezumi, Phys. Plasmas 8 (2001) 3314.
[18] W.A.J. Vijvers, A high-flux cascaded arc hydrogen plasma source (Ph.D. thesis), University of Eindhoven, The Netherlands, 2011.
[19] P.C. Stangeby, The Plasma Boundary of Magnetic Fusion Devices, Taylor & Francis group, London, 2000.
[20] G. De Temmerman, M.A. van den Berg, J. Scholten, A. Lof, H.J. van der Meiden, H.J.N. van Eck, et al., Fusion Eng. Des. 88 (2013) 483.
[21] G. De Temmerman, J. Daniels, K. Bystrov, M.A. van den Berg, J.J. Zielinski, Nucl. Fusion 53 (2013) 023008.
[22] T.W. Morgan, T.M. De Kruif, H.J. van der Meiden, M.A. van den Berg, J. Scholten, W. Melissen, et al., Plasma Phys. Control. Fusion (2014) (in press).
[23] J.J. Zielinski, H.J. van der Meiden, T.W. Morgan, D.C. Schram, G. De Temmerman, Plasma Sources Sci. Technol. 21 (2012) 065003.
[24] F.G. Federici, A. Loarte, G. Strohmayer, Plasma Phys. Control. Fusion 45 (2003) 1523.
[25] A. Loarte, G. Huijsmans, S. Futatani, L.R. Baylor, T.E. Evans, D.M. Orlov, et al., Nucl. Fusion 54 (2014) 033007.
[26] S. Kajita, D. Nishijima, N. Ohno, S. Takamura, J. Appl. Phys. 100 (2006) 103304.
[27] S. Kajita, S. Takamura, N. Ohno, D. Nishijima, H. Iwakiri, N. Yoshida, Nucl. Fusion 47 (2007) 1358.
[28] K.R. Umstadter, R. Doerner, G. Tynan, J. Nucl. Mater. 386–388 (2009) 751.
[29] K.R. Umstadter, R. Doerner, G. Tynan, Phys. Scr. T145 (2011) 014010.
[30] H.W. Kugel, M.G. Bell, J.-W. Ahn, J.P. Allain, R. Bell, J. Boedo, et al., Phys. Plasmas 15 (2008) 056118.